Published for SISSA by Springer

Received: March 22, 2022
Revised: April 13, 2022
Accepted: April 17, 2022
Published: May 17, 2022

JHEP05(2022)108

Search for new hadronic decays of h_c and observation of $h_c \to p\bar{p}\eta$

BESIII

The BESIII collaboration

E-mail: besiii-publications@ihep.ac.cn

Abstract: A search for the hadronic decays of the h_c meson to the final states $p\bar{p}\pi^+\pi^-\pi^0$, $p\bar{p}\eta$, and $p\bar{p}\pi^0$ via the process $\psi(3686) \to \pi^0 h_c$ is performed using $(4.48 \pm 0.03) \times 10^8$ $\psi(3686)$ events collected with the BESIII detector. The decay channel $h_c \to p\bar{p}\eta$ is observed for the first time with a significance greater than 5σ and a branching fraction of $(6.41 \pm 1.74 \pm 0.53 \pm 1.00) \times 10^{-4}$, where the uncertainties are statistical, systematic, and that from the branching fraction of $\psi(3686) \to \pi^0 h_c$. Strong evidence for the decay $h_c \to p\bar{p}\pi^+\pi^-\pi^0$ is found with a significance of 4.9σ and a branching fraction of $(3.84 \pm 0.83 \pm 0.69 \pm 0.58) \times 10^{-3}$. The significances include systematic uncertainties. No clear signal of the decay $h_c \to p\bar{p}\pi^0$ is found, and an upper limit of 6.59×10^{-4} on its branching fraction is set at the 90% confidence level.

Keywords: Branching fraction, e^+-e^- Experiments, Particle and Resonance Production, Quarkonium

ArXiv ePrint: 2203.10439

Corrected publication 2022

https://doi.org/10.1007/JHEP05(2022)108

Contents

1 Introduction 1

2 BESIII detector and Monte Carlo simulation 2

3 Event selection and data analysis 2

4 Result 4

5 Systematic uncertainty 5

6 Summary 8

The BESIII collaboration 13

JHEP05(2022)108

1 Introduction

The study of charmonium states is crucial for a deeper understanding of the low-energy regime of quantum chromodynamics (QCD). All charmonium states below open-charm $D\bar{D}$ threshold have been observed experimentally and can be well described by potential models [1]. However, knowledge about the P-wave spin-singlet, $h_c(^1P_1)$, is still sparse. Theoretically, Kuang considered the effect of $S-D$ mixing and predicted $\mathcal{B}(h_c \to \gamma\eta_c) = (41 \pm 3)\%$ with a non-relativistic QCD model [2], while Godfrey and Rosner predicted $\mathcal{B}(h_c \to \gamma\eta_c) = 38\%$ with a QCD model [3]. Experimentally, the BESIII experiment measured $\mathcal{B}(h_c \to \gamma\eta_c) = (54.3 \pm 6.7 \pm 5.2)\%$, which is close to these predictions, indicating that the electric dipole ($E1$) $h_c \to \gamma\eta_c$ transition is dominant in h_c decay, but that about one half of h_c decays are to non-$E1$ modes. Until now, relatively few non-$E1$ decay modes, which include two radiative decays [4] and some light hadron decays [5–7], have been observed. The sum of all measured branching fractions for h_c non-$E1$ decays is $\sim 3\%$, so there are many unknown h_c decay modes after several decades of research.

The h_c state cannot be directly produced in e^+e^- collisions due to its quantum numbers $J^{PC} = 1^{+-}$. However, it can be produced in charmonium hadronic transitions, e.g., $\psi\,(3686) \to \pi^0 h_c$, whose branching fraction is measured to be $\mathcal{B}(\psi(3686) \to \pi^0 h_c) = (8.4\pm1.3\pm1.0)\times10^{-4}$ [8]. In 2009 and 2012, the BESIII experiment collected $(4.48\pm0.03)\times10^8$ $\psi(3686)$ events [9], which implies that about 0.4 million h_c events are available via $\psi(3686)$ decays, providing a good opportunity to study the nature of the h_c state.

In this paper, we present the first search for the $h_c \to p\bar{p}X$ ($X = \pi^+\pi^-\pi^0$, η, π^0) decays via the $\psi(3686) \to \pi^0 h_c$ process. Hereafter, we denote the three decay modes as mode I, II, and III, respectively.

2 BESIII detector and Monte Carlo simulation

The BESIII detector is a magnetic spectrometer [10] located at the Beijing Electron Positron Collider (BEPCII) [11]. The cylindrical core of the BESIII detector consists of a helium-based multi-layer drift chamber (MDC), a plastic scintillator time-of-flight system (TOF), and a CsI(Tl) electromagnetic calorimeter (EMC), which are all enclosed in a superconducting solenoidal magnet, providing a 1.0 T magnetic field. The solenoid is supported by an octagonal flux-return yoke with resistive plate chamber muon identifier modules interleaved with steel.

The acceptance of charged particles and photons is 93% over the 4π solid angle. The charged-particle momentum resolution at $1\,\mathrm{GeV}/c$ is 0.5%, and the specific energy loss (dE/dx) resolution is 6% for the electrons from Bhabha scattering. The EMC measures photon energies with a resolution of 2.5% (5%) at 1 GeV in the barrel (end cap) region. The time resolution of the TOF barrel section is 68 ps, while that of the end cap section is 110 ps. The end cap TOF system was upgraded in 2015 with multi-gap resistive plate chamber technology, providing a time resolution of 60 ps [12, 13]. About 70% of the data sample used here was taken after this upgrade.

Simulated data samples produced with GEANT4-based [14] Monte Carlo (MC) software, which includes the geometric description of the BESIII detector and the detector response, are used to determine the detection efficiency and to estimate the background contributions. Inclusive MC samples are produced to estimate the contributions from possible background channels. The simulation includes the beam energy spread and initial-state radiation (ISR) in the e^+e^- annihilations modeled with the generator KKMC [15, 16]. The ISR production of vector charmonium(like) states and the continuum processes are also incorporated in KKMC [15, 16]. The known decay modes are modeled with EVTGEN [17, 18], using branching fractions from the PDG [19], and the remaining unknown decays are generated with LUNDCHARM [20]. Final state radiation from charged final state particles is incorporated with PHOTOS [21]. For the exclusive MC simulation samples, the three channels of interest are generated using the phase-space model (PHSP) for each signal mode.

3 Event selection and data analysis

Each charged track reconstructed in the MDC is required to originate from a region of 10 cm from the interaction point (IP) along the z axis, which is the symmetry axis of the MDC, and 1 cm in the plane perpendicular to z. The polar angle θ with respect to the z axis of the tracks must be within the fiducial volume of the MDC, $|\cos\theta| < 0.93$. The measurements of flight time in the TOF and dE/dx in the MDC for each charged track are combined to compute particle identification (PID) confidence levels for pion, kaon and proton hypotheses. The track is assigned to the particle type with the highest confidence level, and that level is required to be greater than 0.001. Finally, a vertex fit constraining all charged tracks to come from a common IP is made.

Photon candidates are reconstructed from isolated electromagnetic showers produced in the crystals of the EMC. A shower is treated as a photon candidate if the deposited energy

JHEP05(2022)108

is larger than 25 MeV in the barrel region ($|\cos\theta| < 0.8$) or 50 MeV in the end cap region ($0.86 < |\cos\theta| < 0.92$). The timing of the shower is required to be within 700 ns from the reconstructed event start time to suppress noise and energy deposits unrelated to the event.

The π^0 candidates are reconstructed from $\gamma\gamma$ combinations with invariant mass within $(0.080,\ 0.200)\,\mathrm{GeV}/c^2$. To improve the momentum resolution and suppress the wrong combination background, a one-constraint (1C) kinematic fit is performed to constrain the $\gamma\gamma$ invariant mass to the nominal π^0 mass [19], and the goodness-of-fit $\chi^2_{1C}(\gamma\gamma)$ is required to be less than 20. The η candidates are reconstructed from $\gamma\gamma$ combinations with invariant mass within $(0.450,\ 0.650)\,\mathrm{GeV}/c^2$, and the invariant mass of the photon pair is constrained to the nominal η mass [19] with a 1C-kinematic fit requiring $\chi^2_{1C}(\gamma\gamma) < 200$.

In order to reduce background events and to improve the mass resolution, a six-constraint (6C) kinematic fit is performed constraining the final state energy-momentum to the total initial four-momentum of the colliding beams, and constraining the masses of the two π^0s to the known π^0 mass in the $h_c \to p\bar{p}\pi^+\pi^-\pi^0$ and $h_c \to p\bar{p}\pi^0$ decays or constraining the masses of the π^0 and η mesons to their known values in the $h_c \to p\bar{p}\eta$ decay. The combination with the smallest value of the 6C-kinematic fit quality χ^2_{6C} is kept for further analysis. The χ^2_{6C} values for $h_c \to p\bar{p}\pi^+\pi^-\pi^0$, $h_c \to p\bar{p}\eta$ and $h_c \to p\bar{p}\pi^0$ decays are required to be less than $45, 45$, and 64, respectively. These values are obtained by optimizing the figure-of-merit (FOM) defined as $S/\sqrt{S+B}$, where S denotes the normalized number of signal events, obtained from MC simulation, while B is the number of background events, obtained from inclusive MC samples.

To suppress contamination from decays with different numbers of photons, such as the dominant decay $\psi(3686) \to \gamma\chi_{c2}$, where the χ_{c2} decays to the same final states as the h_c, $\chi^2_{4C,n\gamma} < \chi^2_{4C,(n-1)\gamma}$ and $\chi^2_{4C,n\gamma} < \chi^2_{4C,(n+1)\gamma}$ are required for each decay mode. Here $\chi_{4C,n\gamma}$ is obtained from a four-constraint (4C) kinematic fit including the expected number of photons n in the signal candidate, while $\chi^2_{4C,(n-1)\gamma}$ and $\chi^2_{4C,(n+1)\gamma}$ are determined from additional 4C fits with one missing or one additional photon compared to the signal process, respectively.

The J/ψ-related background is vetoed by requirements on the $\pi^0\pi^0$, $\pi^+\pi^-$, and η recoil masses. The bachelor π^0 from the decay $\psi(3686) \to \pi^0 h_c$ is identified by its energy being closest to the expected energy, which is determined to be about 0.16 GeV according to $\psi(3686)$ two-body decay. Furthermore, the bachelor π^0 when combined with other final state particles should not be consistent with coming from any resonance. Therefore, additional vetoes are applied to suppress background from $\omega \to \pi^+\pi^-\pi^0$, $\eta \to \pi^+\pi^-\pi^0$, $\Sigma^+ \to p\pi^0$ and $\bar{\Sigma}^- \to \bar{p}\pi^0$, as given in table 1, where M and m denote the invariant mass and the known mass [19] of the indicated particle, respectively; RM denotes the recoiling mass, defined as $RM(X) = \sqrt{\left(p_{\psi(3686)} - p_X\right)^2}$, where $p_{\psi(3686)}$ and p_X are the four momentums of $\psi(3686)$ and X, respectively. The $\Lambda/\bar{\Lambda}$-related background is also suppressed by requiring the invariant mass of $p\pi^-/\bar{p}\pi^+$ to be out of the $\Lambda/\bar{\Lambda}$ mass window, and the K^0_S background is rejected by requiring $m_{\pi^+\pi^-}$ to be out of the K^0_S mass window. All mass windows are obtained by optimizing the FOM and are listed in table 1. No significant intermediate process signal is observed in the study.

JHEP05(2022)108

Mode	Mass Windows [MeV/c^2]
(I)	$\left\|RM(\pi^+\pi^-) - m_{J/\psi}\right\| < 15$
	$\left\|RM(\pi^0\pi^0) - m_{J/\psi}\right\| < 16$
	$\left\|M(\pi^+\pi^-\pi^0) - m_\eta\right\| < 6$
	$M(\pi^+\pi^-\pi^0) \in (762, 802)$
	$M(p\pi^0) \in (1180, 1196)$ &$M(\bar{p}\pi^0) \in (1181, 1194)$
	$M(p\pi^-) \in (1104, 1122)$
	$M(\bar{p}\pi^+) \in (1104, 1122)$
	$M(\pi^+\pi^-) \in (490, 499)$
(II)	$\left\|RM(\eta) - m_{J/\psi}\right\| < 22$
(III)	$\left\|RM(\pi^0\pi^0) - m_{J/\psi}\right\| < 30$
	$M(p\pi^0) \in (1172, 1202)$ &$M(\bar{p}\pi^0) \in (1171, 1202)$

Table 1. Mass windows used as vetoes in each exclusive mode.

After applying all selection criteria, the invariant mass distributions for the three h_c exclusive decay modes are shown in figure 1. Potential background channels from the inclusive MC sample are identified by TopoAna [22], which shows that the remaining background mainly originates from resonant production with the same final state particles as the signal. To investigate possible background from continuum processes, the same selection criteria are applied to a data sample of 44 pb^{-1} collected below the $\psi(3686)$ resonance at $\sqrt{s} = 3.65\,\text{GeV}$. Only a few events survive in modes I and III, but they are outside the h_c signal region.

4 Result

To determine the number of h_c signal events N^{sig} in each decay mode, unbinned maximum likelihood fits are performed to the corresponding mass spectra as shown in figure 1. In all fits, the signal distribution is described by a MC-simulated shape convolved with a Gaussian function accounting for the mass resolution difference between data and MC simulation. The background shape is described by an ARGUS function [23], where the threshold parameter of the ARGUS function is fixed to the kinematical threshold of 3.551 MeV/c^2. The branching fractions of $h_c \to p\bar{p}X$ are determined by

$$\mathcal{B}(h_c \to p\bar{p}X) = \frac{N^{\text{sig}}}{N_{\psi(3686)} \cdot \mathcal{B}(\psi(3686) \to \pi^0 h_c) \cdot \prod_i \mathcal{B}_i \cdot \varepsilon}. \tag{4.1}$$

Here, $\prod_i \mathcal{B}_i$ is the product of branching fractions of the decaying particles like $\mathcal{B}(\pi^0 \to \gamma\gamma)$ and $\mathcal{B}(\eta \to \gamma\gamma)$ taken from the PDG [19]. The number of $\psi(3686)$ events is determined to be $N_{\psi(3686)} = (448.1 \pm 2.9) \times 10^6$ [9]. The detection efficiencies ε are obtained from signal MC simulations, and are determined to be 6.0%, 18.1%, and 23.0% for the three decay modes, respectively.

JHEP05(2022)108

In case of mode II, there are two η decay modes, $\eta \to \gamma\gamma$ and $\eta \to \pi^+\pi^-\pi^0$. A simultaneous unbinned maximum likelihood fit is performed to determine the branching fraction $\mathcal{B}(h_c \to p\bar{p}\eta)$, which is taken as the common parameter among the different decay modes. The corresponding number of h_c signal events in the two different final states is calculated by:

$$N^{\rm sig} = N_{\psi(3686)} \cdot \mathcal{B}\left(\psi\,(3686) \to \pi^0 h_c\right) \cdot \mathcal{B}\left(h_c \to p\bar{p}\eta\right) \cdot \mathcal{B}\left(\pi^0 \to \gamma\gamma\right) \cdot \mathcal{B}\left(\eta \to X\right) \cdot \varepsilon\,. \quad (4.2)$$

For the $\eta \to \gamma\gamma$ mode, an additional normalized peaking background component from $h_c \to \gamma\eta_c, \eta_c \to p\bar{p}\pi^0$ is included. For the $\eta \to \pi^+\pi^-\pi^0$ mode, the accepted candidate events require the invariant mass of $\pi^+\pi^-\pi^0$ to be in the η signal region, i.e., $532 < M_{\pi^+\pi^-\pi^0} < 562\,\mathrm{MeV}/c^2$. The corresponding η side-band shows no obvious peaking background. The numerical results for $\mathcal{B}(h_c \to p\bar{p}X)$ and the resulting branching fraction $\mathcal{B}\left(\psi\,(3686) \to \pi^0 h_c\right) \cdot \mathcal{B}\left(h_c \to p\bar{p}X\right)$ are listed in table 2.

For mode III, no significant signal is observed, and an upper limit on the branching fraction is determined by a Bayesian approach [24]. To obtain the likelihood distribution, the signal yield is scanned using the fit function, eq. (4.1). Systematic uncertainties are considered by smearing the obtained likelihood curve with a Gaussian function with the width of the systematic uncertainty of the respective decay mode. The upper limit at the 90% confidence level on the number of events $N^{\rm up}_{h_c}$ is determined by integrating the smeared likelihood function $\mathcal{L}(N)$ up to the value $N^{\rm up}_{hc}$, which corresponds to 90% of the integral,

$$0.9 = \frac{\int_0^{N^{\rm up}_{h_c}} dN\mathcal{L}(N)}{\int_0^{\infty} dN\mathcal{L}(N)}\,. \quad (4.3)$$

The results are listed in table 2 and 3.

Among the three h_c decay modes, mode I is observed with a statistical significance of 5.1 standard deviations (σ). The significance for mode II is also determined to be 5.1σ by combining the two η decay modes, while the significance of mode III is 1σ. The statistical significance is estimated by the likelihood difference between the fits with and without signal component, taking the change in the degrees of freedom into account. To evaluate the effect of the systematic uncertainty on the signal significance, we repeat the fits with variations of the signal shape, background shape, and fit range, and find the statistical significance of mode II to be always larger than 5σ, and mode I to be larger than 4.9σ.

5 Systematic uncertainty

The sources of systematic uncertainties for the branching fractions include tracking, photon detection, π^0 reconstruction, PID, the kinematic fit, mass windows, fitting procedure, the branching fraction of the intermediate decay, the number of $\psi(3686)$ events and the physics model describing the h_c production and decay dynamics. All the systematic uncertainties are summarized in table 4 for modes I and III, and in table 5 for mode II. The overall systematic uncertainty for the product branching $\mathcal{B}(\psi(3686) \to \pi^0 h_c) \cdot \mathcal{B}(h_c \to p\bar{p}X)$ is obtained by summing all individual components in quadrature. The third uncertainty

JHEP05(2022)108

Mode	I	III
$p\bar{p}X$	$p\bar{p}\pi^+\pi^-\pi^0$	$p\bar{p}\pi^0$
N_{h_c}	86.5 ± 18.7	< 57
$\mathcal{B}(h_c \to p\bar{p}X)$	$(3.84 \pm 0.83 \pm 0.69 \pm 0.58) \times 10^{-3}$	$< 6.59 \times 10^{-4}$
$\mathcal{B}(\psi(3686) \to \pi^0 h_c) \times \mathcal{B}(h_c \to p\bar{p}X)$	$(3.30 \pm 0.71 \pm 0.59) \times 10^{-6}$	$< 5.67 \times 10^{-7}$
Significance(σ)	4.9	—

Table 2. The number of observed signal events N_{h_c}, the absolute branching fraction $\mathcal{B}(h_c \to p\bar{p}X)$, the product branching fraction $\mathcal{B}(\psi(3686) \to \pi^0 h_c) \times \mathcal{B}(h_c \to p\bar{p}X)$, and the statistical significance, including systematic uncertainties. Here, the first uncertainty is statistical, the second is systematic, and the third one arises from the branching fraction of $\psi(3686) \to \pi^0 h_c$ [19].

Mode	II	
$p\bar{p}\eta$	$\eta \to \pi^+\pi^-\pi^0$	$\eta \to \gamma\gamma$
N_{h_c}	3.4 ± 0.9	18.1 ± 4.9
$\mathcal{B}(h_c \to p\bar{p}\eta)$	$(6.41 \pm 1.74 \pm 0.53 \pm 1.00) \times 10^{-4}$	
$\mathcal{B}(\psi(3686) \to \pi^0 h_c) \times \mathcal{B}(h_c \to p\bar{p}\eta)$	$(5.51 \pm 1.50 \pm 0.46) \times 10^{-7}$	
Significance(σ)	5.1	

Table 3. The number of observed signal events N_{h_c}, the absolute branching fraction $\mathcal{B}(h_c \to p\bar{p}\eta)$, the product branching fraction $\mathcal{B}(\psi(3686) \to \pi^0 h_c) \times \mathcal{B}(h_c \to p\bar{p}\eta)$, and the statistical significance, including systematic uncertainties.

for $\mathcal{B}(h_c \to p\bar{p}X)$ of $\Delta_{\rm ext} = 15.1\%$ is due to the uncertainty of the branching fraction of $\psi(3686) \to \pi^0 h_c$ [19].

- **Tracking efficiency and photon detection.** The uncertainties of the tracking efficiency are estimated with the control samples $J/\psi \to p\bar{p}\pi^+\pi^-$ and $\psi(3686) \to p\bar{p}\pi^+\pi^-$, and are determined to be 1.0% [25], 1.3%, and 1.7% [6] for each charged pion, proton and antiproton, respectively. The uncertainty of the detection efficiency of photons is studied using the control sample $J/\psi \to \pi^+\pi^-\pi^0$, and is determined to be 1.0% per photon [26].

- **π^0 and η reconstruction efficiencies.** There are two π^0 candidates with different momentum distributions for mode I and III, while there is only one π^0 candidate in mode II. The uncertainties of the two π^0 reconstructions differ due to the different momentum distributions. The corresponding uncertainties for the three decay modes are determined to be $0.6\%, 0.3\%, 1.8\%$, respectively. The uncertainty due to η reconstruction from $\gamma\gamma$ final states is determined by using a high purity control sample of $J/\psi \to \eta p\bar{p}$ decays [26]. The difference of η reconstruction efficiency between data and MC simulation gives an uncertainty of 1% per η.

- **PID.** The uncertainty due to PID is determined to be 1.0% per pion [27], 1.3% per proton, and 1.6% per antiproton, based on the same samples used to estimate tracking

JHEP05(2022)108

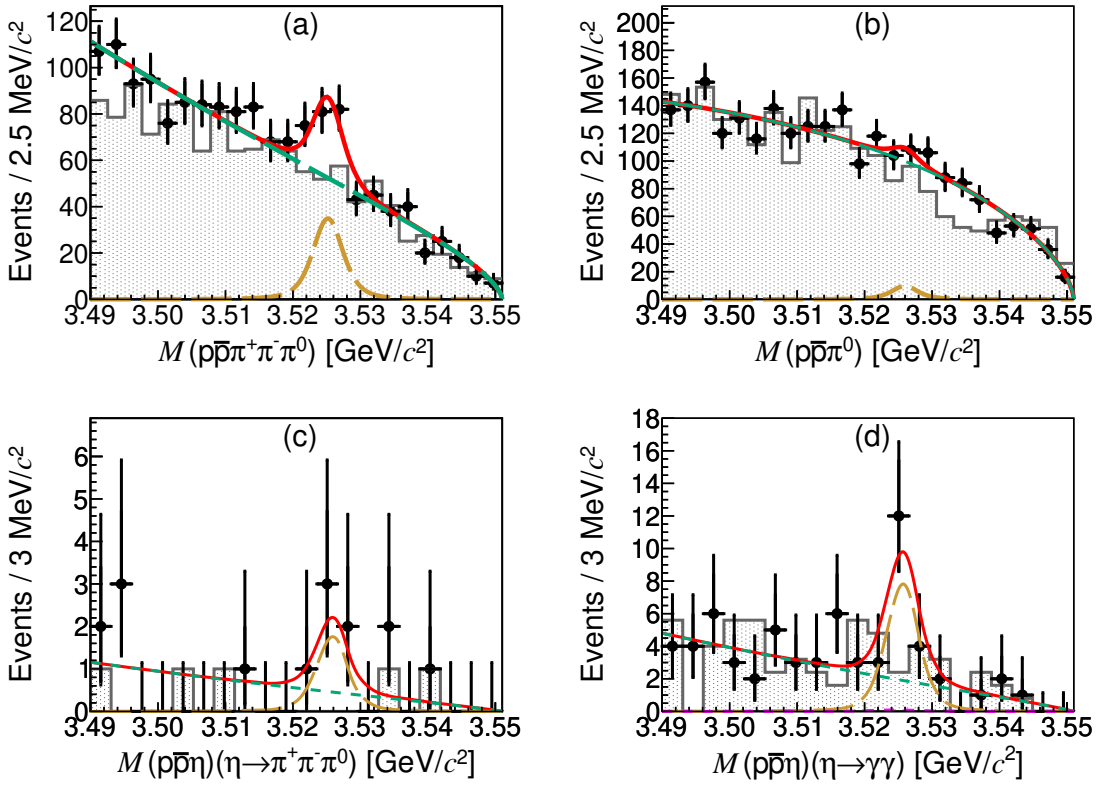

Figure 1. Fits to the invariant mass spectra of (a) $p\bar{p}\pi^+\pi^-\pi^0$ and (b) $p\bar{p}\pi^0$ and simultaneous fits to the invariant mass spectra of (c) $p\bar{p}\eta$ with $\eta\to\pi^+\pi^-\pi^0$ and (d) $\eta\to\gamma\gamma$ for data. Data are shown as points with error bars, the total fit result is shown by the red solid line, the background contribution is denoted by the green dashed line (including the peaking background contribution shown barely discernible in pink in (d)), and the signal contribution is illustrated by the gold dashed line. The background obtained from inclusive MC samples is shown by the gray shaded histogram.

efficiencies [6]. Tables 4 and 5 list the relative systematic uncertainties due to PID for the different decay modes.

- **Kinematic fit.** The uncertainties associated with the kinematic fit are studied with the track helix parameter correction method, as described in ref. [28]. In the standard analysis, these corrections are applied. The difference of the MC signal efficiencies without corrected track parameters are taken as the corresponding systematic uncertainties.

- **Mass windows.** The uncertainties associated with the mass windows are estimated by repeating the analysis with alternative mass window requirements. The largest differences from the nominal branching fractions are assigned as the corresponding systematic uncertainties. In addition, the systematic uncertainties due to the $\Lambda/\bar{\Lambda}, \Sigma^+/\bar{\Sigma}^-$ mass window requirements are estimated by the control samples, $\psi(3686)\to\Lambda\bar{\Lambda}\pi^0\pi^0$ and $\psi(3686)\to\Sigma\bar{\Sigma}\pi^+\pi^-$, respectively. The differences of the selection efficiencies between data and MC simulation from control samples are taken as the corresponding systematic uncertainties.

JHEP05(2022)108

- **Fit range.** The uncertainty due to the fitting range is obtained by changing the range by $\pm 0.01\,\mathrm{GeV}/c^2$, and the largest difference in the branching fraction is taken as the systematic uncertainty.

- **Signal shape.** The uncertainty due to signal shape is estimated by replacing the MC-simulated shape convolved with a Gaussian function by only the MC-simulated shape. The difference in the measured branching fraction is taken as the systematic uncertainty.

- **Background shape.** The uncertainties caused by the background shape are estimated by alternatively using different shapes. For mode I, we use an MC-simulated shape which is obtained by an MC sample of $\psi(3686) \to ph_1(1170)\bar{\Delta}^+ + c.c.$ and $\psi(3686) \to \Delta^{++}\,\Delta^{--}\pi^0\pi^0$, to replace the ARGUS function. For mode II, we use a 2^{nd}-order Chebychev polynomial to replace the nominal ARGUS function. The differences in the measured branching fractions are taken as the systematic uncertainties. The uncertainty due to $\eta \to \gamma\gamma$ peaking background in mode II is taken from the uncertainty on the branching fraction. For mode III, we use the ARGUS function to replace the nominal MC-simulated shape.

- **Intermediate decays.** The maximum deviations from the known branching fractions are taken as systematic uncertainties as listed in tables 4 and 5.

- $\boldsymbol{N_{\psi(3686)}}$**.** The uncertainties due to the number of $\psi(3686)$ events ($N_{\psi(3686)}$) are determined with inclusive hadronic $\psi(3686)$ decays and estimated to be 0.7% [9].

- **Physics model.** The systematic uncertainties due to the physics model come from two sources, the unknown intermediate states in $h_c \to$ hadrons, and the decay $\psi(3686) \to \pi^0 h_c$. Since there is little knowledge of h_c state decay dynamics and limited statistics in this analysis, we estimate the uncertainty due to possible intermediate resonances by including additional intermediate states, and the results are compared with those of the nominal phase space sample. For the uncertainties due to the physics model of $\psi(3686) \to \pi^0 h_c$, we take the efficiency differences between the signal MC generated from PHSP and the HELAMP model [17, 18] as the systematic uncertainties. The uncertainties for the three decay modes are determined to be 2.4%, 0.7%, 0.4%, respectively.

Tables 4 and 5 summarize all the systematic uncertainties of the different decay modes. The overall systematic uncertainties are obtained by adding all systematic uncertainties in quadrature assuming they are independent. For mode II, there are two η decay channels. Therefore, the uncommon items are determined using the weighted average of the detection efficiency and the branching fraction of the subsequent decays in individual decay modes [29].

6 Summary

Using a data sample of $(448.1 \pm 2.9) \times 10^6$ $\psi(3686)$ events collected with the BESIII detector, three decay modes of the h_c have been searched for. The decay channel $h_c \to p\bar{p}\eta$ is

JHEP05(2022)108

Source	$h_c \to p\bar{p}\pi^+\pi^-\pi^0$	$h_c \to p\bar{p}\pi^0$
Tracking	5.0	3.0
Photon detection	4.0	4.0
π^0 reconstruction	0.6	1.8
PID	4.9	2.9
Kinematic fit	1.0	0.4
Mass windows	12.5	7.4
Fit range	5.3	1.6
Signal shape	4.4	3.6
Background shape	6.8	2.3
Intermediate decay	Negligible	Negligible
$N_{\psi(3686)}$	0.7	0.7
Physics model	2.4	0.7
Sum	18.0	10.6

Table 4. The relative systematic uncertainties for the $h_c \to p\bar{p}\pi^+\pi^-\pi^0$, $p\bar{p}\pi^0$ decay channels (in %).

Source	$\eta \to \gamma\gamma$	$\eta \to \pi^+\pi^-\pi^0$
Tracking	3.0	5.0
Photon detection	4.0	
η reconstruction	1.0	—
π^0 reconstruction	0.2	0.6
PID	2.9	4.9
Kinematic fit	0.4	1.0
η_c peaking background	1.5	—
Intermediate decay	0.5	1.2
veto $\psi\,(3686) \to \eta J/\psi$	4.5	—
Physics model	0.2	1.7
Fitting range	3.7	
Signal shape	0.9	
Background shape	0.2	
$N_{\psi(3686)}$	0.7	
Sum	8.3	

Table 5. The relative systematic uncertainties for the $h_c \to p\bar{p}\eta$ channel (in %). A dash indicates that the systematic uncertainty is not applicable.

JHEP05(2022)108

observed for the first time with a 5.1σ statistical significance, and evidence for the decay $h_c \to p\bar{p}\pi^+\pi^-\pi^0$ is found with a statistical significance of 4.9σ. No obvious signal for $h_c \to p\bar{p}\pi^0$ is seen. The product branching fractions, $\mathcal{B}(\psi(3686) \to \pi^0 h_c) \times \mathcal{B}(h_c \to p\bar{p}X)$, and the absolute branching fractions, $\mathcal{B}(h_c \to p\bar{p}X)$, are listed in table 2. The branching fractions obtained in this analysis are at the level of $\sim 10^{-3}$, which is the same level as the previously observed decays of $h_c \to 2(\pi^+\pi^-)\pi^0$, $p\bar{p}\pi^+\pi^-$ [6] and $h_c \to K^+K^-\pi^+\pi^-\pi^0$, $\pi^+\pi^-\pi^0\eta$, $K^0_S K^\pm\pi^\mp\pi^+\pi^-$ [7]. These measurements are essential to test the theoretical prediction [2]. Finally, it is still unclear whether the hadronic decay width of the h_c is of the same order as the radiative decay width predicted in [30]. Future experimental measurements searching for more decay modes based on the larger data set of $\psi(3686)$ events [31], together with improved theoretical calculations can help us to answer this question.

Acknowledgments

The BESIII collaboration thanks the staff of BEPCII and the IHEP computing center for their strong support. This work is supported in part by National Key Basic Research Program of China under Contracts Nos. 2020YFA0406300, 2020YFA0406400; National Natural Science Foundation of China (NSFC) under Contracts Nos. 11605042, 11625523, 11635010, 11735014, 11822506, 11835012, 11875122, 11935015, 11935016, 11935018, 11905236, 11961141012, 12022510, 12025502, 12035009, 12035013, 1204750, 12075107, 12061131003; the Chinese Academy of Sciences (CAS) Large-Scale Scientific Facility Program; Joint Large-Scale Scientific Facility Funds of the NSFC and CAS under Contracts Nos. U1732263, U1832207; CAS Key Research Program of Frontier Sciences under Contract No. QYZDJ-SSW-SLH040; 100 Talents Program of CAS; INPAC and Shanghai Key Laboratory for Particle Physics and Cosmology; ERC under Contract No. 758462; European Union Horizon 2020 research and innovation programme under Contract No. Marie Sklodowska-Curie grant agreement No 894790; German Research Foundation DFG under Contracts Nos. 443159800, Collaborative Research Center CRC 1044, FOR 2359, GRK 214; Istituto Nazionale di Fisica Nucleare, Italy; Ministry of Development of Turkey under Contract No.DPT2006K-120470; National Science and Technology fund; Olle Engkvist Foundation under Contract No. 2000605; STFC (United Kingdom); The Knut and Alice Wallenberg Foundation (Sweden) under Contract No.2016.0157; The Royal Society, U.K. under Contracts Nos. DH140054, DH160214; The Swedish Research Council; U. S. Department of Energy under Contracts Nos. DE-FG02-05ER41374, DE-SC-0012069; Excellent Youth Foundation of Henan Province under Contracts No. 212300410010; The youth talent support program of Henan Province under Contracts No. ZYQR201912178.

JHEP05(2022)108

References

[1] T. Barnes, S. Godfrey and E.S. Swanson, *Higher charmonia*, *Phys. Rev. D* **72** (2005) 054026 [hep-ph/0505002] [INSPIRE].

[2] Y.-P. Kuang, *S-D mixing and searching for the $\psi(3686)(1^1P_1)$ state at the Beijing Electron-Positron Coolider*, *Phys. Rev. D* **65** (2002) 094024 [hep-ph/0201210] [INSPIRE].

[3] S. Godfrey and J.L. Rosner, *Production of singlet P wave $c\bar{c}$ and $b\bar{b}$ states*, *Phys. Rev. D* **66** (2002) 014012 [hep-ph/0205255] [INSPIRE].

[4] BESIII collaboration, *Observation of h_c radiative decay $h_c \to \gamma\eta'$ and evidence for $h_c \to \gamma\eta$*, *Phys. Rev. Lett.* **116** (2016) 251802 [arXiv:1603.04936] [INSPIRE].

[5] CLEO collaboration, *Evidence for decays of h_c to multipion final states*, *Phys. Rev. D* **80** (2009) 051106 [arXiv:0906.4470] [INSPIRE].

[6] BESIII collaboration, *First observations of $h_c \to$ hadrons*, *Phys. Rev. D* **99** (2019) 072008 [arXiv:1810.12023] [INSPIRE].

[7] BESIII collaboration, *Search for New Hadronic Decays of h_c and Observation of $h_c \to K^+K^-\pi^+\pi^-\pi^0$*, *Phys. Rev. D* **102** (2020) 112007 [arXiv:2010.12092] [INSPIRE].

[8] BESIII collaboration, *Measurements of $h_c(^1P_1)$ in ψ' Decays*, *Phys. Rev. Lett.* **104** (2010) 132002 [arXiv:1002.0501] [INSPIRE].

[9] BESIII collaboration, *Determination of the number of $\psi(3686)$ events at BESIII*, *Chin. Phys. C* **42** (2018) 023001 [arXiv:1709.03653] [INSPIRE].

[10] BESIII collaboration, *Design and Construction of the BESIII Detector*, *Nucl. Instrum. Meth. A* **614** (2010) 345 [arXiv:0911.4960] [INSPIRE].

[11] C.H. Yu et al., *BEPCII Performance and Beam Dynamics Studies on Luminosity*, in proceedings of *7th International Particle Accelerator Conference (IPAC2016)*, Busan, Republic of Korea, 8–13 May 2016, JACoW, Geneva Swizerland (2016), https://accelconf.web.cern.ch/ipac2016/doi/JACoW-IPAC2016-TUYA01.html [INSPIRE].

[12] X. Li et al., *Study of MRPC technology for BESIII endcap-TOF upgrade*, *Rad. Det. Tech. Meth.* **1** (2017) 13.

[13] Y.X. Guo et al., *The study of time calibration for upgraded end cap TOF of BESIII*, *Radiat. Detect. Technol. Meth.* **1** (2017) 15.

[14] GEANT4 collaboration, *GEANT4 — a simulation toolkit*, *Nucl. Instrum. Meth. A* **506** (2003) 250 [INSPIRE].

[15] S. Jadach, B.F.L. Ward and Z. Was, *The Precision Monte Carlo event generator KK for two fermion final states in e^+e^- collisions*, *Comput. Phys. Commun.* **130** (2000) 260 [hep-ph/9912214] [INSPIRE].

[16] S. Jadach, B.F.L. Ward and Z. Was, *Coherent exclusive exponentiation for precision Monte Carlo calculations*, *Phys. Rev. D* **63** (2001) 113009 [hep-ph/0006359] [INSPIRE].

[17] R.-G. Ping, *Event generators at BESIII*, *Chin. Phys. C* **32** (2008) 599 [INSPIRE].

[18] D.J. Lange, *The EvtGen particle decay simulation package*, *Nucl. Instrum. Meth. A* **462** (2001) 152 [INSPIRE].

[19] Particle Data Group collaboration, *Review of Particle Physics*, *PTEP* **2020** (2020) 083C01 [INSPIRE].

JHEP05(2022)108

[20] J.C. Chen, G.S. Huang, X.R. Qi, D.H. Zhang and Y.S. Zhu, *Event generator for J/ψ and $\psi(2S)$ decay*, *Phys. Rev. D* **62** (2000) 034003 [INSPIRE].

[21] E. Richter-Was, *QED bremsstrahlung in semileptonic B and leptonic τ decays*, *Phys. Lett. B* **303** (1993) 163 [INSPIRE].

[22] X. Zhou, S. Du, G. Li and C. Shen, *TopoAna: A generic tool for the event type analysis of inclusive Monte-Carlo samples in high energy physics experiments*, *Comput. Phys. Commun.* **258** (2021) 107540 [arXiv:2001.04016] [INSPIRE].

[23] ARGUS collaboration, *Measurement of the polarization in the decay $B \to J/\psi K^*$*, *Phys. Lett. B* **340** (1994) 217 [INSPIRE].

[24] G.J. Feldman and R.D. Cousins, *A Unified approach to the classical statistical analysis of small signals*, *Phys. Rev. D* **57** (1998) 3873 [physics/9711021] [INSPIRE].

[25] W.-L. Yuan, X.-C. Ai, X.-B. Ji, S.-J. Chen, Y. Zhang, L.-H. Wu et al., *Study of tracking efficiency and its systematic uncertainty from $J/\psi \to p\bar{p}\pi^+\pi^-$ at BESIII*, *Chin. Phys. C* **40** (2016) 026201 [arXiv:1507.03453] [INSPIRE].

[26] BESIII collaboration, *Branching fraction measurements of χ_{c0} and χ_{c2} to $\pi^0\pi^0$ and $\eta\eta$*, *Phys. Rev. D* **81** (2010) 052005 [arXiv:1001.5360] [INSPIRE].

[27] BESIII collaboration, *Study of $\psi(3686) \to \pi^0 h_c$, $h_c \to \gamma\eta_c$ via η_c exclusive decays*, *Phys. Rev. D* **86** (2012) 092009 [arXiv:1209.4963] [INSPIRE].

[28] BESIII collaboration, *Search for hadronic transition $\chi_{cJ} \to \eta_c\pi^+\pi^-$ and observation of $\chi_{cJ} \to K\overline{K}\pi\pi\pi$*, *Phys. Rev. D* **87** (2013) 012002 [arXiv:1208.4805] [INSPIRE].

[29] BESIII collaboration, *Observation of $\chi_{c2} \to \eta'\eta'$ and $\chi_{c0,2} \to \eta\eta'$*, *Phys. Rev. D* **96** (2017) 112006 [arXiv:1707.07042] [INSPIRE].

[30] G.T. Bodwin, E. Braaten and G.P. Lepage, *Rigorous QCD predictions for decays of P wave quarkonia*, *Phys. Rev. D* **46** (1992) R1914 [hep-lat/9205006] [INSPIRE].

[31] BESIII collaboration, *Future Physics Programme of BESIII*, *Chin. Phys. C* **44** (2020) 040001 [arXiv:1912.05983] [INSPIRE].

JHEP05(2022)108

The BESIII collaboration

M. Ablikim[1], M.N. Achasov[10,b], P. Adlarson[68], S. Ahmed[14], M. Albrecht[4], R. Aliberti[28], A. Amoroso[67A,67C], M.R. An[32], Q. An[64,50], X.H. Bai[58], Y. Bai[49], O. Bakina[29], R. Baldini Ferroli[23A], I. Balossino[24A], Y. Ban[39,h], K. Begzsuren[26], N. Berger[28], M. Bertani[23A], D. Bettoni[24A], F. Bianchi[67A,67C], J. Bloms[61], A. Bortone[67A,67C], I. Boyko[29], R.A. Briere[5], H. Cai[69], X. Cai[1,50], A. Calcaterra[23A], G.F. Cao[1,55], N. Cao[1,55], S.A. Cetin[54A], J.F. Chang[1,50], W.L. Chang[1,55], G. Chelkov[29,a], G. Chen[1], H.S. Chen[1,55], M.L. Chen[1,50], S.J. Chen[35], X.R. Chen[25], Y.B. Chen[1,50], Z.J. Chen[20,i], W.S. Cheng[67C], G. Cibinetto[24A], F. Cossio[67C], J.J. Cui[42], X.F. Cui[36], H.L. Dai[1,50], J.P. Dai[71], X.C. Dai[1,55], A. Dbeyssi[14], R. E. de Boer[4], D. Dedovich[29], Z.Y. Deng[1], A. Denig[28], I. Denysenko[29], M. Destefanis[67A,67C], F. De Mori[67A,67C], Y. Ding[33], C. Dong[36], J. Dong[1,50], L.Y. Dong[1,55], M.Y. Dong[1,50,55], X. Dong[69], S.X. Du[73], P. Egorov[29,a], Y.L. Fan[69], J. Fang[1,50], S.S. Fang[1,55], Y. Fang[1], R. Farinelli[24A], L. Fava[67B,67C], F. Feldbauer[4], G. Felici[23A], C.Q. Feng[64,50], J.H. Feng[51], M. Fritsch[4], C.D. Fu[1], Y. Gao[64,50], Y. Gao[39,h], I. Garzia[24A,24B], P.T. Ge[69], C. Geng[51], E.M. Gersabeck[59], A Gilman[62], K. Goetzen[11], L. Gong[33], W.X. Gong[1,50], W. Gradl[28], M. Greco[67A,67C], L.M. Gu[35], M.H. Gu[1,50], C. Y Guan[1,55], A.Q. Guo[22], A.Q. Guo[25], L.B. Guo[34], R.P. Guo[41], Y.P. Guo[9,f], A. Guskov[29,a], T.T. Han[42], W.Y. Han[32], X.Q. Hao[15], F.A. Harris[57], K.K. He[47], K.L. He[1,55], F.H. Heinsius[4], C.H. Heinz[28], Y.K. Heng[1,50,55], C. Herold[52], M. Himmelreich[11,d], T. Holtmann[4], G.Y. Hou[1,55], Y.R. Hou[55], Z.L. Hou[1], H.M. Hu[1,55], J.F. Hu[48,j], T. Hu[1,50,55], Y. Hu[1], G.S. Huang[64,50], L.Q. Huang[65], X.T. Huang[42], Y.P. Huang[1], Z. Huang[39,h], T. Hussain[66], N Hüsken[22,28], W. Ikegami Andersson[68], W. Imoehl[22], M. Irshad[64,50], S. Jaeger[4], S. Janchiv[26], Q. Ji[1], Q.P. Ji[15], X.B. Ji[1,55], X.L. Ji[1,50], Y.Y. Ji[42], H.B. Jiang[42], X.S. Jiang[1,50,55], J.B. Jiao[42], Z. Jiao[18], S. Jin[35], Y. Jin[58], M.Q. Jing[1,55], T. Johansson[68], N. Kalantar-Nayestanaki[56], X.S. Kang[33], R. Kappert[56], M. Kavatsyuk[56], B.C. Ke[44,1], I.K. Keshk[4], A. Khoukaz[61], P. Kiese[28], R. Kiuchi[1], R. Kliemt[11], L. Koch[30], O.B. Kolcu[54A], B. Kopf[4], M. Kuemmel[4], M. Kuessner[4], A. Kupsc[37,68], M. G. Kurth[1,55], W. Kühn[30], J.J. Lane[59], J.S. Lange[30], P. Larin[14], A. Lavania[21], L. Lavezzi[67A,67C], Z.H. Lei[64,50], H. Leithoff[28], M. Lellmann[28], T. Lenz[28], C. Li[40], C.H. Li[32], Cheng Li[64,50], D.M. Li[73], F. Li[1,50], G. Li[1], H. Li[44], H. Li[64,50], H.B. Li[1,55], H.J. Li[15], H.N. Li[48,j], J.L. Li[42], J.Q. Li[4], J.S. Li[51], Ke Li[1], L.K. Li[1], Lei Li[3], P.R. Li[31,k,l], S.Y. Li[53], W.D. Li[1,55], W.G. Li[1], X.H. Li[64,50], X.L. Li[42], Xiaoyu Li[1,55], Z.Y. Li[51], H. Liang[1,55], H. Liang[27], H. Liang[64,50], Y.F. Liang[46], Y.T. Liang[25], G.R. Liao[12], L.Z. Liao[1,55], J. Libby[21], A. Limphirat[52], C.X. Lin[51], D.X. Lin[25], T. Lin[1], B.J. Liu[1], C.X. Liu[1], D. Liu[14,64], F.H. Liu[45], Fang Liu[1], Feng Liu[6], G.M. Liu[48,j], H.M. Liu[1,55], Huanhuan Liu[1], Huihui Liu[16], J.B. Liu[64,50], J.L. Liu[65], J.Y. Liu[1,55], K. Liu[1], K.Y. Liu[33], Ke Liu[17,m], L. Liu[64,50], M.H. Liu[9,f], P.L. Liu[1], Q. Liu[69], Q. Liu[55], S.B. Liu[64,50], T. Liu[1,55], T. Liu[9,f], W.M. Liu[64,50], X. Liu[31,k,l], Y. Liu[31,k,l], Y.B. Liu[36], Z.A. Liu[1,50,55], Z.Q. Liu[42], X.C. Lou[1,50,55], F.X. Lu[51], H.J. Lu[18], J.D. Lu[1,55], J.G. Lu[1,50], X.L. Lu[1], Y. Lu[1], Y.P. Lu[1,50], C.L. Luo[34], M.X. Luo[72], P.W. Luo[51], T. Luo[9,f], X.L. Luo[1,50], X.R. Lyu[55], F.C. Ma[33], H.L. Ma[1], L.L. Ma[42], M.M. Ma[1,55], Q.M. Ma[1], R.Q. Ma[1,55], R.T. Ma[55], X.X. Ma[1,55], X.Y. Ma[1,50], Y. Ma[39,h], F.E. Maas[14], M. Maggiora[67A,67C], S. Maldaner[4], S. Malde[62], Q.A. Malik[66], A. Mangoni[23B], Y.J. Mao[39,h], Z.P. Mao[1], S. Marcello[67A,67C], Z.X. Meng[58], J.G. Messchendorp[56], G. Mezzadri[24A], T.J. Min[35], R.E. Mitchell[22], X.H. Mo[1,50,55], N. Yu. Muchnoi[10,b], H. Muramatsu[60], S. Nakhoul[11,d], Y. Nefedov[29], F. Nerling[11,d], I.B. Nikolaev[10,b], Z. Ning[1,50], S. Nisar[8,g], S.L. Olsen[55], Q. Ouyang[1,50,55], S. Pacetti[23B,23C], X. Pan[9,f], Y. Pan[59], A. Pathak[1], A. Pathak[27], P. Patteri[23A], M. Pelizaeus[4], H.P. Peng[64,50], K. Peters[11,d], J. Pettersson[68], J.L. Ping[34], R.G. Ping[1,55], S. Plura[28], S. Pogodin[29], R. Poling[60], V. Prasad[64,50], H. Qi[64,50], H.R. Qi[53], M. Qi[35], T.Y. Qi[9,f], S. Qian[1,50], W.B. Qian[55], Z. Qian[51], C.F. Qiao[55], J.J. Qin[65], L.Q. Qin[12], X.P. Qin[9,f], X.S. Qin[42], Z.H. Qin[1,50], J.F. Qiu[1], S.Q. Qu[36], K.H. Rashid[66], K. Ravindran[21], C.F. Redmer[28], A. Rivetti[67C], V. Rodin[56], M. Rolo[67C], G. Rong[1,55], Ch. Rosner[14], M. Rump[61], H.S. Sang[64], A. Sarantsev[29,c], Y. Schelhaas[28],

JHEP05(2022)108

C. Schnier[4], K. Schoenning[68], M. Scodeggio[24A,24B], W. Shan[19], X.Y. Shan[64,50], J.F. Shangguan[47], M. Shao[64,50], C.P. Shen[9,f], H.F. Shen[1,55], X.Y. Shen[1,55], H.C. Shi[64,50], R.S. Shi[1,55], X. Shi[1,50], X. D Shi[64,50], J.J. Song[15], W.M. Song[27,1], Y.X. Song[39,h], S. Sosio[67A,67C], S. Spataro[67A,67C], F. Stieler[28], K.X. Su[69], P.P. Su[47], G.X. Sun[1], H.K. Sun[1], J.F. Sun[15], L. Sun[69], S.S. Sun[1,55], T. Sun[1,55], W.Y. Sun[27], X Sun[20,i], Y.J. Sun[64,50], Y.Z. Sun[1], Z.T. Sun[1], Y.H. Tan[69], Y.X. Tan[64,50], C.J. Tang[46], G.Y. Tang[1], J. Tang[51], Q.T. Tao[20,i], J.X. Teng[64,50], V. Thoren[68], W.H. Tian[44], Y.T. Tian[25], I. Uman[54B], B. Wang[1], C.W. Wang[35], D.Y. Wang[39,h], H.J. Wang[31,k,l], H.P. Wang[1,55], K. Wang[1,50], L.L. Wang[1], M. Wang[42], M.Z. Wang[39,h], Meng Wang[1,55], S. Wang[9,f], W. Wang[51], W.H. Wang[69], W.P. Wang[64,50], X. Wang[39,h], X.F. Wang[31,k,l], X.L. Wang[9,f], Y. Wang[51], Y.D. Wang[38], Y.F. Wang[1,50,55], Y.Q. Wang[1,55], Y.Y. Wang[31,k,l], Z. Wang[1,50], Z.Y. Wang[1,55], Ziyi Wang[55], Zongyuan Wang[1,55], D.H. Wei[12], F. Weidner[61], S.P. Wen[1], D.J. White[59], U. Wiedner[4], G. Wilkinson[62], M. Wolke[68], L. Wollenberg[4], J.F. Wu[1,55], L.H. Wu[1], L.J. Wu[1,55], X. Wu[9,f], X.H. Wu[27], Z. Wu[1,50], L. Xia[64,50], T. Xiang[39,h], H. Xiao[9,f], S.Y. Xiao[1], Z.J. Xiao[34], X.H. Xie[39,h], Y.G. Xie[1,50], Y.H. Xie[6], T.Y. Xing[1,55], C.J. Xu[51], G.F. Xu[1], Q.J. Xu[13], W. Xu[1,55], X.P. Xu[47], Y.C. Xu[55], F. Yan[9,f], L. Yan[9,f], W.B. Yan[64,50], W.C. Yan[73], H.J. Yang[43,e], H.X. Yang[1], L. Yang[44], S.L. Yang[55], Y.X. Yang[12], Yifan Yang[1,55], Zhi Yang[25], M. Ye[1,50], M.H. Ye[7], J.H. Yin[1], Z.Y. You[51], B.X. Yu[1,50,55], C.X. Yu[36], G. Yu[1,55], J.S. Yu[20,i], T. Yu[65], C.Z. Yuan[1,55], L. Yuan[2], Y. Yuan[1], Z.Y. Yuan[51], C.X. Yue[32], A.A. Zafar[66], X. Zeng Zeng[6], Y. Zeng[20,i], A.Q. Zhang[1], B.X. Zhang[1], G.Y. Zhang[15], H. Zhang[64], H.H. Zhang[27], H.H. Zhang[51], H.Y. Zhang[1,50], J.L. Zhang[70], J.Q. Zhang[34], J.W. Zhang[1,50,55], J.Y. Zhang[1], J.Z. Zhang[1,55], Jianyu Zhang[1,55], Jiawei Zhang[1,55], L.M. Zhang[53], L.Q. Zhang[51], Lei Zhang[35], S. Zhang[51], S.F. Zhang[35], Shulei Zhang[20,i], X.D. Zhang[38], X.M. Zhang[1], X.Y. Zhang[42], Y. Zhang[62], Y.T. Zhang[73], Y.H. Zhang[1,50], Yan Zhang[64,50], Yao Zhang[1], Z.Y. Zhang[69], G. Zhao[1], J. Zhao[32], J.Y. Zhao[1,55], J.Z. Zhao[1,50], Lei Zhao[64,50], Ling Zhao[1], M.G. Zhao[36], Q. Zhao[1], S.J. Zhao[73], Y.B. Zhao[1,50], Y.X. Zhao[25], Z.G. Zhao[64,50], A. Zhemchugov[29,a], B. Zheng[65], J.P. Zheng[1,50], Y.H. Zheng[55], B. Zhong[34], C. Zhong[65], L.P. Zhou[1,55], Q. Zhou[1,55], X. Zhou[69], X.K. Zhou[55], X.R. Zhou[64,50], X.Y. Zhou[32], A.N. Zhu[1,55], J. Zhu[36], K. Zhu[1], K.J. Zhu[1,50,55], L. Zhu[15], S.H. Zhu[63], T.J. Zhu[70], W.J. Zhu[36], W.J. Zhu[9,f], Y.C. Zhu[64,50], Z.A. Zhu[1,55], B.S. Zou[1], J.H. Zou[1]

[1] *Institute of High Energy Physics, Beijing 100049, People's Republic of China*
[2] *Beihang University, Beijing 100191, People's Republic of China*
[3] *Beijing Institute of Petrochemical Technology, Beijing 102617, People's Republic of China*
[4] *Bochum Ruhr-University, D-44780 Bochum, Germany*
[5] *Carnegie Mellon University, Pittsburgh, Pennsylvania 15213, U.S.A.*
[6] *Central China Normal University, Wuhan 430079, People's Republic of China*
[7] *China Center of Advanced Science and Technology, Beijing 100190, People's Republic of China*
[8] *COMSATS University Islamabad, Lahore Campus, Defence Road, Off Raiwind Road, 54000 Lahore, Pakistan*
[9] *Fudan University, Shanghai 200443, People's Republic of China*
[10] *G.I. Budker Institute of Nuclear Physics SB RAS (BINP), Novosibirsk 630090, Russia*
[11] *GSI Helmholtzcentre for Heavy Ion Research GmbH, D-64291 Darmstadt, Germany*
[12] *Guangxi Normal University, Guilin 541004, People's Republic of China*
[13] *Hangzhou Normal University, Hangzhou 310036, People's Republic of China*
[14] *Helmholtz Institute Mainz, Staudinger Weg 18, D-55099 Mainz, Germany*
[15] *Henan Normal University, Xinxiang 453007, People's Republic of China*
[16] *Henan University of Science and Technology, Luoyang 471003, People's Republic of China*
[17] *Henan University of Technology, Zhengzhou 450001, People's Republic of China*
[18] *Huangshan College, Huangshan 245000, People's Republic of China*
[19] *Hunan Normal University, Changsha 410081, People's Republic of China*
[20] *Hunan University, Changsha 410082, People's Republic of China*

JHEP05(2022)108

[21] Indian Institute of Technology Madras, Chennai 600036, India
[22] Indiana University, Bloomington, Indiana 47405, U.S.A.
[23] INFN Laboratori Nazionali di Frascati, (A)INFN Laboratori Nazionali di Frascati, I-00044, Frascati, Italy; (B)INFN Sezione di Perugia, I-06100, Perugia, Italy; (C)University of Perugia, I-06100, Perugia, Italy
[24] INFN Sezione di Ferrara, (A)INFN Sezione di Ferrara, I-44122, Ferrara, Italy; (B)University of Ferrara, I-44122, Ferrara, Italy
[25] Institute of Modern Physics, Lanzhou 730000, People's Republic of China
[26] Institute of Physics and Technology, Peace Ave. 54B, Ulaanbaatar 13330, Mongolia
[27] Jilin University, Changchun 130012, People's Republic of China
[28] Johannes Gutenberg University of Mainz, Johann-Joachim-Becher-Weg 45, D-55099 Mainz, Germany
[29] Joint Institute for Nuclear Research, 141980 Dubna, Moscow region, Russia
[30] Justus-Liebig-Universitaet Giessen, II. Physikalisches Institut, Heinrich-Buff-Ring 16, D-35392 Giessen, Germany
[31] Lanzhou University, Lanzhou 730000, People's Republic of China
[32] Liaoning Normal University, Dalian 116029, People's Republic of China
[33] Liaoning University, Shenyang 110036, People's Republic of China
[34] Nanjing Normal University, Nanjing 210023, People's Republic of China
[35] Nanjing University, Nanjing 210093, People's Republic of China
[36] Nankai University, Tianjin 300071, People's Republic of China
[37] National Centre for Nuclear Research, Warsaw 02-093, Poland
[38] North China Electric Power University, Beijing 102206, People's Republic of China
[39] Peking University, Beijing 100871, People's Republic of China
[40] Qufu Normal University, Qufu 273165, People's Republic of China
[41] Shandong Normal University, Jinan 250014, People's Republic of China
[42] Shandong University, Jinan 250100, People's Republic of China
[43] Shanghai Jiao Tong University, Shanghai 200240, People's Republic of China
[44] Shanxi Normal University, Linfen 041004, People's Republic of China
[45] Shanxi University, Taiyuan 030006, People's Republic of China
[46] Sichuan University, Chengdu 610064, People's Republic of China
[47] Soochow University, Suzhou 215006, People's Republic of China
[48] South China Normal University, Guangzhou 510006, People's Republic of China
[49] Southeast University, Nanjing 211100, People's Republic of China
[50] State Key Laboratory of Particle Detection and Electronics, Beijing 100049, Hefei 230026, People's Republic of China
[51] Sun Yat-Sen University, Guangzhou 510275, People's Republic of China
[52] Suranaree University of Technology, University Avenue 111, Nakhon Ratchasima 30000, Thailand
[53] Tsinghua University, Beijing 100084, People's Republic of China
[54] Turkish Accelerator Center Particle Factory Group, (A)Istinye University, 34010, Istanbul, Turkey; (B)Near East University, Nicosia, North Cyprus, Mersin 10, Turkey
[55] University of Chinese Academy of Sciences, Beijing 100049, People's Republic of China
[56] University of Groningen, NL-9747 AA Groningen, The Netherlands
[57] University of Hawaii, Honolulu, Hawaii 96822, U.S.A.
[58] University of Jinan, Jinan 250022, People's Republic of China
[59] University of Manchester, Oxford Road, Manchester, M13 9PL, United Kingdom
[60] University of Minnesota, Minneapolis, Minnesota 55455, U.S.A.
[61] University of Muenster, Wilhelm-Klemm-Str. 9, 48149 Muenster, Germany
[62] University of Oxford, Keble Rd, Oxford, OX13RH, U.K.
[63] University of Science and Technology Liaoning, Anshan 114051, People's Republic of China
[64] University of Science and Technology of China, Hefei 230026, People's Republic of China
[65] University of South China, Hengyang 421001, People's Republic of China
[66] University of the Punjab, Lahore-54590, Pakistan

JHEP05(2022)108

[67] University of Turin and INFN, (A)University of Turin, I-10125, Turin, Italy; (B)University of Eastern Piedmont, I-15121, Alessandria, Italy; (C)INFN, I-10125, Turin, Italy
[68] Uppsala University, Box 516, SE-75120 Uppsala, Sweden
[69] Wuhan University, Wuhan 430072, People's Republic of China
[70] Xinyang Normal University, Xinyang 464000, People's Republic of China
[71] Yunnan University, Kunming 650500, People's Republic of China
[72] Zhejiang University, Hangzhou 310027, People's Republic of China
[73] Zhengzhou University, Zhengzhou 450001, People's Republic of China

[a] Also at the Moscow Institute of Physics and Technology, Moscow 141700, Russia
[b] Also at the Novosibirsk State University, Novosibirsk, 630090, Russia
[c] Also at the NRC "Kurchatov Institute", PNPI, 188300, Gatchina, Russia
[d] Also at Goethe University Frankfurt, 60323 Frankfurt am Main, Germany
[e] Also at Key Laboratory for Particle Physics, Astrophysics and Cosmology, Ministry of Education; Shanghai Key Laboratory for Particle Physics and Cosmology; Institute of Nuclear and Particle Physics, Shanghai 200240, People's Republic of China
[f] Also at Key Laboratory of Nuclear Physics and Ion-beam Application (MOE) and Institute of Modern Physics, Fudan University, Shanghai 200443, People's Republic of China
[g] Also at Harvard University, Department of Physics, Cambridge, MA, 02138, U.S.A.
[h] Also at State Key Laboratory of Nuclear Physics and Technology, Peking University, Beijing 100871, People's Republic of China
[i] Also at School of Physics and Electronics, Hunan University, Changsha 410082, China
[j] Also at Guangdong Provincial Key Laboratory of Nuclear Science, Institute of Quantum Matter, South China Normal University, Guangzhou 510006, China
[k] Also at Frontiers Science Center for Rare Isotopes, Lanzhou University, Lanzhou 730000, People's Republic of China
[l] Also at Lanzhou Center for Theoretical Physics, Lanzhou University, Lanzhou 730000, People's Republic of China
[m] Henan University of Technology, Zhengzhou 450001, People's Republic of China

JHEP05(2022)108